6th World Conference on Experimental Heat Transfer, Fluid Mechanics, and Thermodynamics
April 17-21, 2005, Matsushima, Miyagi, Japan

Three-dimensional vortical structures in a coaxial jet manipulated with micro-actuators

K. P. Angele, N. Kurimoto, Y. Suzuki and N. Kasagi

The University of Tokyo, Tokyo 113-8656, Japan
E-mail : angele@thtlab.t.u-tokyo.ac.jp

ABSTRACT

The development of three-dimensional vortical structures was investigated in order to shed some light on the mixing enhancement mechanism in a controlled coaxial jet. Detailed measurements of secondary azimuthal instabilities and streamwise vortices were achieved by applying stereoscopic PIV to the cross-stream plane of the jet. It was found that non-axisymetric forcing modes, in particular the least stable helical mode, renders earlier development of streamwise vortices as compared to forcing with the axi-symmetric mode. However, the number of streamwise vortices increases in the downstream direction for all control modes and eventually approaches a similar level, roughly given by twice the azimuthal wavenumber. The streamwise vortices were found to be equal in size and strength to the primary vortices. This fact emphasizes their significance in the jet dynamics and their potential for mixing. Comparing with the results from a mixing measurement made earlier in the present setup [15], it can be concluded that, for the natural coaxial jet and the axi-symmetrically forced jet, the presence of primary vortices, the appearance of streamwise vortices and the onset of mixing, are strongly connected. This leads us to conjecture that non-axisymmetric modes are more beneficial for mixing enhancement.

Keywords *: Streamwise vortices, mixing enhancement, flow control, coaxial jet, PIV*

1. INTRODUCTION

In small-scale distributed energy systems, which are the motivation for the present study, flexible mixing enhancement is required due to the inherently low Reynolds number. Here, a coaxial jet consisting of air and methane, which is a part of a combustor model, is experimentally investigated. The ultimate goal is to generate a system in which the flow structures and the mixing can be flexibly controlled under large load fluctuations.

1.1 Review

The development of two-dimensional and three-dimensional vortical structures and its connection to mixing has been extensively investigated in the past in the generic case of the plane mixing-layer. A mixing-layer with an inflectional velocity profile is unstable which leads to roll-up of Kelvin-Helmholz (KH) vortices. Small differences in the upstream conditions are amplified by the strain in the braid region between the KH vortices and three-dimensional instabilities subsequently lead to the evolution of streamwise vortices before the breakdown to turbulence, see [1].

[2] employed a chemical reaction technique to quantify the mixing in the plane mixing layer, and concluded that mixing transition is a consequence of the onset of small-scale three-dimensional structures. A sinuous “wiggle-disturbance” in the spanwise direction, with a wavelength similar to that of the primary KH vortices, was observed. The amplitude of the disturbance grew in the downstream direction but the length scales remained unchanged. The primary KH vortices remained two-dimensional despite the presence of the wiggle disturbance. The origin of the instability was hypothesized to be either due to the vortex-ring instability, [3], or a Reyleigh-Taylor instability.

The stability problem for the plane mixing-layer was solved numerically as an eigenvalue problem by [4]. They found a spanwise instability, which was named the “translative instability”. The spanwise wavelength was found to be 2/3 of that of the primary KH vortices.

Flow visualizations in the plane mixing-layer were conducted by [5]. These showed that the spanwise wavelength between the streamwise vortices was independent of the Reynolds number, the velocity ratio, the density ratio and the initial shear layer velocity profile shape. The relation between the spanwise and the streamwise wavelengths were found to vary between 0.45 and 1.1, with a mean value of 0.67, in agreement with the predictions by [4]. It was concluded that the streamwise vortices play an important role in the process of mixing.

Flow vizualizations in the plane mixing-layer were also conducted by [6]. It was suggested that spanwise vorticity in the braid region is tilted and stretched into a pair of streamwise vortices. It was observed that the number of streamwise vortices increased in the downstream direction, which was explained by self-induction, stretching and tilting. It was also found that streamwise vortices could develop before the primary KH vortices, depending on the upstream conditions. The spanwise wavelength was found to be slightly smaller than that of the primary KH vortices.

The evolution of primary vortices, secondary instabilities and streamwise vortices is not restricted to the plane mixing-layer. Temporal inviscid vortex filament simulations of a single jet subjected to axial and helical perturbations were carried out by [7,8]. Counter-rotating streamwise vortices, similar to those in the plane mixing-layer, were observed in the first case. In the latter case, the initial helical distutrbance was amplified and formed streamwise vortices of the same sign.

The single jet was experimentally investigated by [9]. Flow visualizations showed fingers in the azimuthal direction and the mode number increased with the Reynolds number. Streamwise

vortices developed and the relative importance of those, with respect to the primary vortex rings, increased in the downstream direction. Two-component PIV was used to estimate the entrainment in the jet.

It was shown by [16] that for a single natural jet, the axi-symmetric mode is the least stable if the ratio between the jet radius and the momentum loss thickness is larger than 6.5 at the end of the potential core, otherwise the helical mode is the least stable mode.

The coaxial jet was extensively investigated in an experiment by [10]. The results showed the importance of the velocity ratio between the two streams for the dynamics of the vortical structures in the near field. Experiments in a coaxial jet were also reported by [11] and it was concluded that there is a critical velocity ratio, above which a transition into a region of backflow at the nozzle exit occurs. Mixing measurements were further reported by [12] from the same setup and streamwise vortices could clearly be observed in the shear layers.

With the development of Micro Electro Mechanical System (MEMS) techniques, which enables the manufacturing of miniature actuators and sensors, flow control for various purposes have become feasible. Helical forcing of a single jet for stabilization of a lifted flame, using piezo-electrical flaps, was recently reported by [13]. Azimuthal fingers were observed but only one streamwise vortex developed.

The possibilities to compute more complex flows and higher Reynolds numbers are constantly increasing in direct numerical simulations (DNS). Inherent in such is more detailed information about the formation and behavior of vortical structures. Another benefit is the relative simplicity with which one can carry out complex flow control, which is not feasible in an experiment. A DNS of a coaxial jet was recently reported by [14]. The helical mode developed and evidence of streamwise vortices was shown in instantaneous realizations of the flow field. The data indicate that the criterion for the least stable mode given by [16] holds also for coaxial jets.

With the recent development of Particle Image Velocimetry (PIV), accurate flow field measurements have become an alternative to qualitative flow visualizations and single-point measurement techniques. The largest benefit of PIV is its ability to measure one component of the vorticity vector, which makes it an excellent tool for measurements of vortical flow structures. It was shown earlier in the present setup, by combining PIV and Laser Induced Fluorescence (LIF) in the downstream-radial plane, that for the axi-symmetric mode, a Strouhal number of unity maximize the number of primary vortex rings and the mixing enhancement in the near field of the coaxial jet, [15]. Most of the mixing takes place between x/D_0=0.5 and x/D_0=1, where D_0 is the outer jet diameter at the nozzle exit, see Fig. 2.

1.2 The present study

In the present study, stereoscopic PIV measurements are conducted in the cross-stream plane of the controlled and the natural cold coaxial jet. Such measurements give a unique way of exploring non-axisymmetric control modes and quantitatively study instantaneous differences in secondary azimuthal instabilities and streamwise vortices. This is utterly useful for increasing the understanding of the mixing mechanism.

2. EXPERIMENT

2.1 Coaxial jet facility

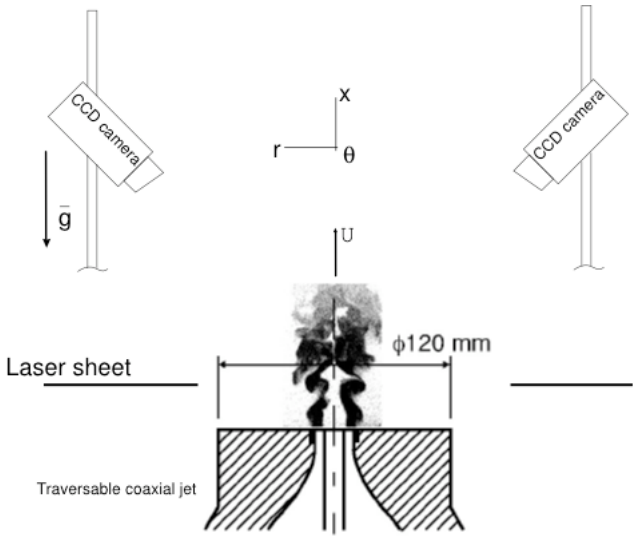

Figure 1. The coaxial jet setup, the stereoscopic PIV arrangement and the coordinate system.

The experimental setup is shown in Fig. 1. The coaxial jet consists of a central methane jet surrounded by an outer air jet issuing into the ambient surrounding air. The Reynolds number, based on D_0=20 mm, and the outer jet bulk velocity, U_b=1.8 m/s, is 2400. The central jet has a diameter of D_i=10 mm and the flow is fully developed laminar. The maximum inlet velocity in the outer jet is U_0=2.4 m/s and the outer-inner velocity ratio is five. The flowrates are carefully controlled by mass-flowmeters.

The least stable mode depends on the shape of the velocity profile and therefore also the shape of the nozzle from which the jet issues. The contraction ratio of the outer jet nozzle is 25 and according to the criteria given by [16], the helical mode is the least stable mode here.

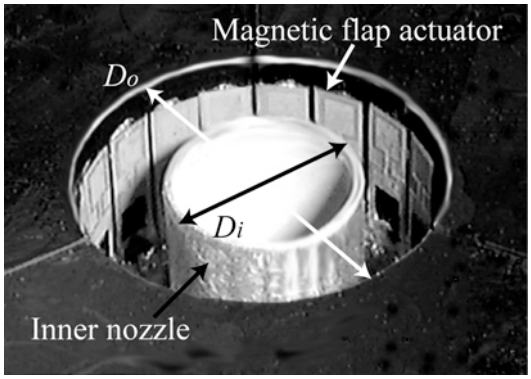

Figure 2. Micro flap-actuator nozzle, D_0=20mm, D_i=10 mm.

Using MEMS techniques, we have developed a configuration,

which consists of 18 individually-driven micro flap actuators, [20], positioned on the periphery of the outer jet nozzle exit, equally spaced in the circumferential direction, see Fig. 2. Employing these, large-scale vortical structures in the outer shear layer can be flexibly manipulated.

As opposed to acoustic forcing, the present configuration allows one to monitor not only the amplitude and frequency but also the disturbance mode. In the present experiments a flap-forcing frequency corresponding to a Strouhal number (based on D_0 and U_b) of unity was used for all the forcing modes, inspired by the results of [15]. With the present flow conditions and experimental setup this corresponds to a frequency of 90 Hz. The different modes investigated are the axi-symmetric mode, the helical mode and a mode we call the alternate mode, where nine flaps are driven out-of-phase with the other nine, creating two half vortex rings, see [20]. The natural jet is also measured.

2.2 PIV setup

The jet setup itself is traversable which implies that the cameras only require to be calibrated once. The angle between the CCD cameras was 90 degrees in order to maximize the accuracy in the out-of-plane component. The cameras contain 1024 x 1280 pixels and were equipped with Nikkor f105 lenses operating at f/11. The image size was designed to enable the whole jet to be captured. The size of an interrogation area (IA) is 0.68 mm.

[17] showed that random errors due to poor light intensity became significant once the light intensity was below 4 bits out of 8 bit resolution. The 400 mJ double-pulsed Thales laser, in combination with a distance of about 500 mm between the laser sheet and the cameras, ensured that the light intensity in the images was sufficient.

The seeding used for the PIV measurements consists of solid SiO_2 particles with a diameter of 1.2 micron. The number of particles inside each IA is above the recommended value of five, [19], to assure a good performance of the correlation technique.

The particle image diameter was above two pixels, and a Gaussian peak-fit was used for the sub-pixel interpolation, in order to minimize peak-locking effects, see [17] and [18].

The images were captured and evaluated by a commercial software by LaVision. The software also handles the calibration of the stereoscopic PIV. The images were evaluated with an adaptive multi-grid algorithm with window-offset, a normalized second order correlation and a deformed IA of 32 x 32 pixels final size. An overlap of 50% of the IA was used in all cross-correlations.

As a means of detecting spurious vectors it is common to use the so-called Peak Value Ratio (PVR), the ratio between the highest and the second highest peaks in the correlation plane. A criterion recommended by [19] is to set a limit at PVR=1.2. This was used here together with a range-validation, discarding all velocities larger than the maximum inlet velocity. The valid detection rate (VDR) is varying between about 90% and 95%. Outliers were replaced by interpolation and subsequently a smoothing of the velocity field was applied prior to computing velocity gradients of the flow field.

The present measurements are a major challenge since the main flow is normal to the laser sheet, posing large restrictions on the parameters determining the accuracy. The laser sheet thickness was slightly broadened to 1.5 mm in order to allow for a larger timing to be used and to increase the effective seeding density. The timing between the two image pairs was 150 micro-seconds. Comparisons between the cross-stream plane PIV measurements and PIV measurements conducted in the radial-downstream direction, see Fig. 4, were made. The agreement for the streamwise component was very good, whereas the radial component, which is much smaller in magnitude, showed some minor differences. 500 image pairs were captured and subjected to averaging in all the cross-stream plane measurements.

3. RESULTS AND DISCUSSION

3.1 Primary vortical structures induced by the flap control

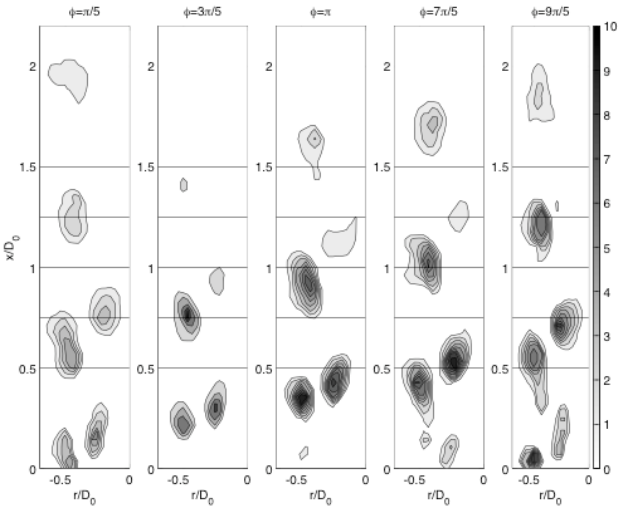

Figure 3. Contours in the xr-plane of the normalized (using D_0 and U_0) phase-averaged second invariant of the velocity gradient tensor in the case of axi-symmetric forcing.

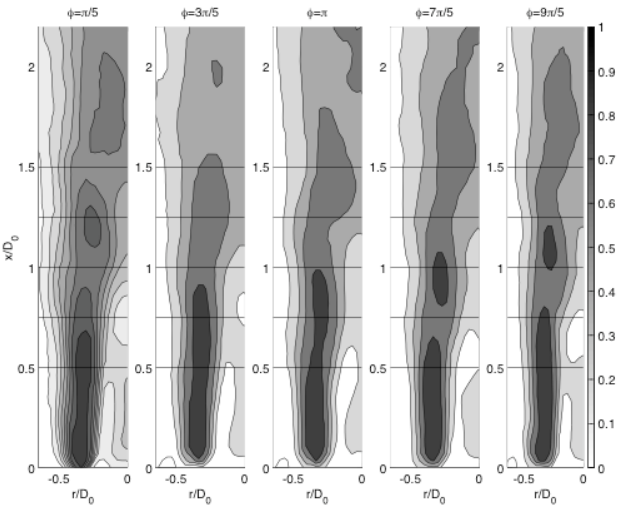

Figure 4. The normalized (with U_0) phase-averaged streamwise velocity in the xr-plane in the case of axi-symmetric forcing.

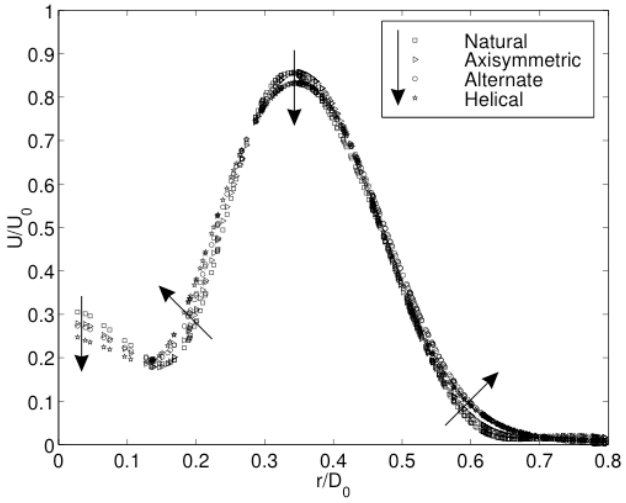

Figure 5 The normalized streamwise mean velocity profiles in the radial direction at x/D_0=0.5 for all the different forcing modes and the natural jet. The data are cross-stream planes averaged in the azimuthal direction.

The present cross-stream plane measurements are concentrated to the region of mixing, see [15], and are indicated by horizontal lines in Fig. 3 and Fig. 4. However, before turning our attention to the cross-stream plane measurements we present the flow field in the radial-downstream direction for the case of axi-symmetric forcing. As is evident from Fig. 3, large-scale primary vortex rings shed synchronized with the frequency of the flaps. The vortices are strong and coherent in the jet near field before breakdown into turbulence. The streamwise wavelength between the vortices originating from two subsequent flap-cycles is approximately 0.5D_0. At this large momentum flux ratio the development of the inner shear layer is governed by the characteristics of the outer shear layer and vortices roll up also in the inner shear layer, [10]. The outer and inner vortices appear in a weakly staggered counter-rotating pattern. The mean radial positions of the vortex rings coincide approximately with the inflection points in the mean velocity profile and the peaks in the velocity fluctuations in the respective shear-layers.

The presence of the vortex-rings distorts the streamline-pattern in the downstream direction, see Fig. 4. As a consequence, the size of the jet and the magnitude of the streamwise velocity, at a certain streamwise position, are strong functions of the phase-angle, most notable in the central jet around x/D_0=0.75.

As the natural coaxial jet develops downstream, the outer jet spreads in the radial direction due to entrainment of the central and the ambient fluid. The maximum velocity in the outer jet decreases as a consequence of this. Initially, the velocity in the central jet also decreases, however, further downstream, it increases and in the far field the coaxial jet resembles the structure of a single jet. Figure 5 shows that, when controlled by the non-axisymmetric modes, the mean velocity profile develops faster, in the above sense, than in the case of axi-symmetric forcing, however, all the forced cases develop faster than the natural jet. This indicates that mixing is promoted by the forcing and suggests that the non-axisymmetric forcing modes lead to a better near field mixing. From the cross-stream plane measurements further downstream, it becomes evident that all the modes develop into the helical mode. The differences in the mean velocity profiles in the near field, shown in Fig. 5, decrease as a consequence of this.

3.2 Secondary instabilities and streamwise vortices

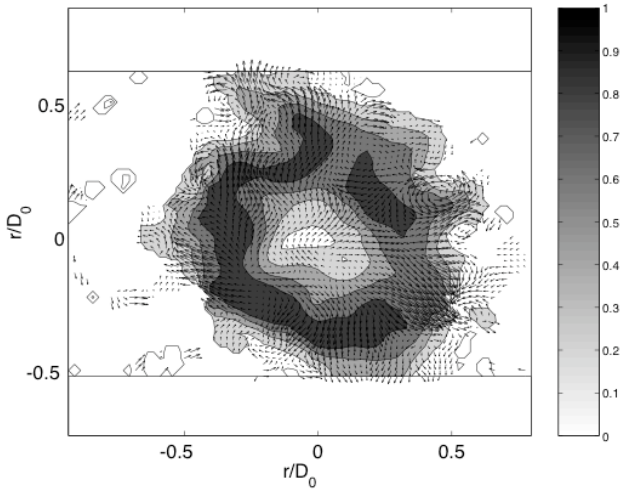

Figure 6. The instantaneous cross-stream plane structure of the jet at x/D_0=1 in the case of the axisymmetric forcing mode.

We now turn to the instantaneous structure of the jet in the cross-stream plane. Figure 6 shows an instantaneous snap-shot of the flow in the cross-stream plane at x/D_0=1 when forced with the axi-symmetric mode. The background contour corresponds to the magnitude of the normalized streamwise velocity, in the same way as in Fig. 4, and the velocity vectors indicate the instantaneous in-plane velocity components. As can be seen, the shear layer between the outer jet and the ambient fluid, as well as that between the outer and the central jets, show secondary azimuthal instabilities, which appear as wiggles in the contour of the streamwise velocity in this plane. Instantaneous realizations of the flow field, such as this one, show that pairs of counter-rotating streamwise vortices evolve from secondary shear layer instabilities in the azimuthal direction, in line with what has been observed in earlier studies of the mixing layers and jets.

3.2.1 Secondary azimuthal instabilities

The wave number spectrum in the azimuthal direction was computed at the positions of the inner and the outer shear-layers, where the velocity fluctuations are largest in magnitude and the primary vortices are positioned. Figure 7 shows that the most energetic aziumthal wave number in the outer shear-layer is around five to six for both the axi-symmetric case and the natural jet. This gives an azimuthal wavelength of about 0.5D_0, i.e. similar to the streamwise ditto, which is in line with the observations from earlier studies. In the inner shear-layer, the most energetic wave number is about half, however, the circumference is also half, which means that the characteristic wavelength is the same. As is evident from Fig. 7, the energy in

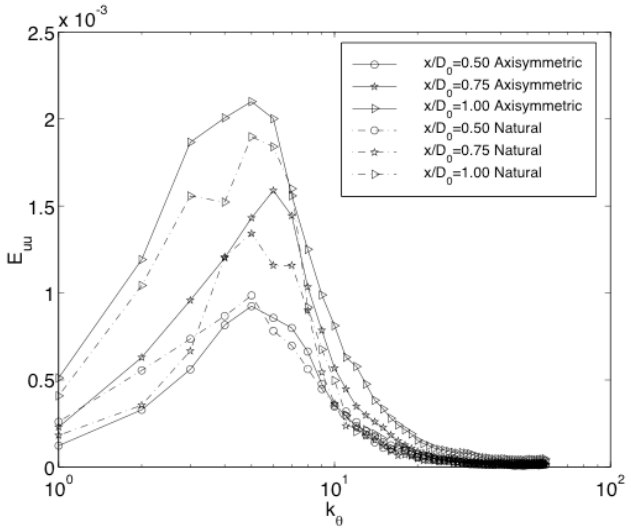

Figure 7. Azimuthal wave-number spectra in the outer shear-layer for the axi-symmetric mode and the natural jet.

the azimuthal instabilities increase in the downstream direction in both the natural and the controlled cases but the wavelength is unchanged. The energy in the outer shear-layer, in the axi-symmetric case, increases faster than in the natural jet due to the forcing, however, the inner shear layer is virtually unchanged in this respect. The energy in the inner shear-layer is overall lower.

3.2.2 Streamwise vortices

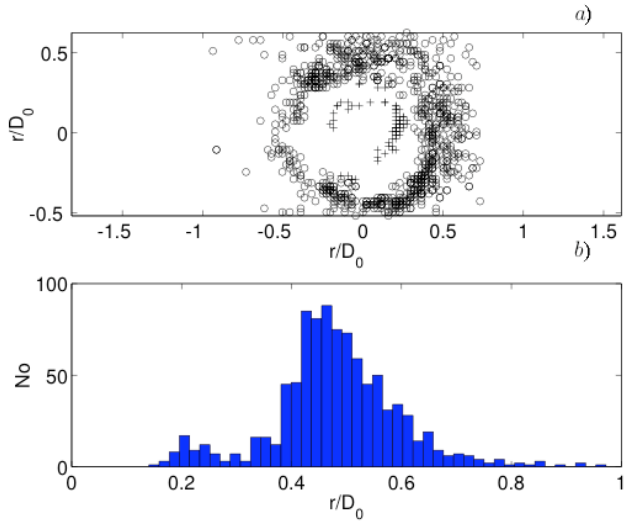

Figure 8. (a) Streamwise vortices populating the outer (o) and the inner (+) shear layers at x/D_0=1, in the case of axis-symmetric forcing. Each symbol corresponds to the position of a streamwise vortex. The data from 100 instantaneous velocity fields were used to construct this figure. (b) The radial probability density function of the data in (a).

In order to detect instantaneous streamwise vortices we use the second invariant of the velocity gradient tensor, assuming that the vortices are perpendicular to the cross-stream plane. A local maximum was taken as the position of a streamwise vortex and the maximum value was taken as the strength of the vortex, Q. The local region around the position of the vortex, where the rotation was larger than a threshold value (10% of the mean strength of the primary vortex rings in the case of axi-symmetric forcing), was used as an estimate of its size, d. Figure 8 shows an example of how streamwise vortices populate the inner and the outer shear layers. The inner shear-layer contains fewer vortices than the outer, due to the limited space. The vortices in the outer shear layer show a larger spread in both size and strength than those in the inner shear layer, see Fig. 9.

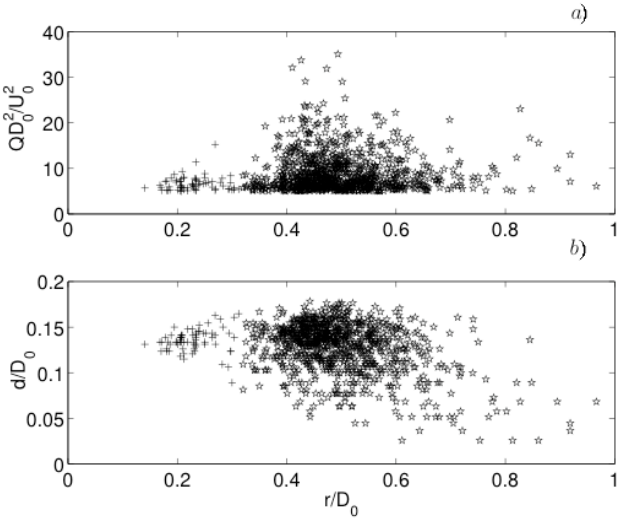

Figure 9. (a) The strength and (b) the size of the streamwise vortices depicted in Fig. 8.

The downstream development of the average number of vortices, the average vortex size, and their average strength, are compared for the different control modes in Fig. 10. In the natural jet, strong streamwise vortices are practically absent in the near field but appear somewhere between x/D_0=1 and x/D_0=1.25, approximately where the primary KH vortices begin to roll up. In all the controlled cases, streamwise vortices populate the shear layer before x/D_0=0.5. Fig 10 (a) shows that the average number of streamwise vortices increases significantly in the downstream direction, as observed by [6]. The development of the streamwise vortices is earlier for the non-axisymmetric modes, in particular for the helical mode. This is in line with the early development of the streamwise mean velocity profile. However, for all the control modes, the amount of vortices approaches a similar level at x/D_0=1.25, roughly given by twice the azimuthal wave number. One might speculate that also the natural jet approaches this level, however, the present measurements do not cover this range.

The average strength and size of the streamwise vortices, shown in Fig 10 (b,c), also increase in the downstream direction, the latter being comparable to the shear layer thickness. The spread of the jet in the downstream direction might explain the slight increase in the average vortex size. The strength of the vortices show a similar trend with respect to the forcing mode, however, it is not as pronounced as for <No>, whereas the size appears to be insensitive to the type of forcing mode and similar

to that of the natural jet. When comparing the strength and size of the streamwise vortices from Fig 10 (b,c) to Fig. 3, it becomes evident that the streamwise vortices are similar in size and strength to the primary vortex rings, which emphasize their significance in the jet dynamics and their potential for mixing enhancement.

The inner shear layer differs significantly from the outer shear layer only in that the amount of vortices is smaller.

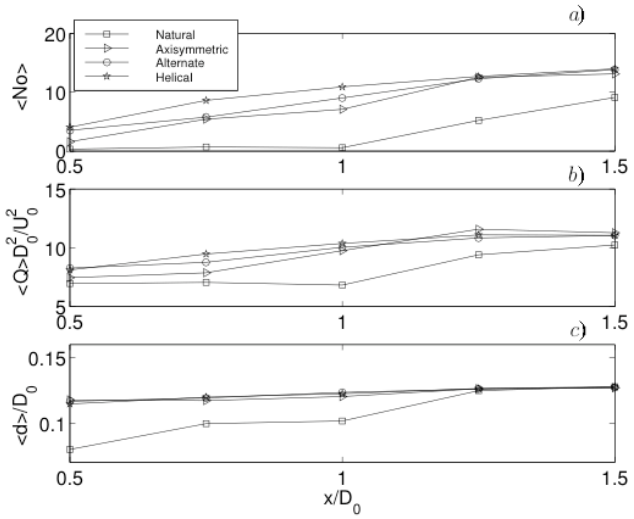

Figure 10 Comparison of the downstream development of the streamwise vortices in the outer shear layer for the different control modes and the natural coaxial jet. (a) The average amount (b) strength and (c) size.

3.3 Mixing enhancement and streamwise vortices

Comparing the results from Fig. 10 to the results from [15], one observes a strong connection between the onset of mixing, the presence of primary vortices and the appearance of secondary streamwise vortical structures in both the natural jet and the controlled jet for a Strouhal number of unity. This leads us to believe that the mixing in the near field of the jet is even more enhanced when using non-axisymmetric forcing modes.

3.3 Future work

PLIF measurements in the cross-stream plane for the non-axisymmetric modes are currently under preparation in order to examine if non-axisymmetric modes are more beneficial for mixing enhancement.

Further investigations of other non-axisymmetric control modes are also being carried out. Preliminary results from control using an inclined vortex ring indicate that it is possible to create an even larger amount of streamwise vortices in the near field of the jet than in the case of helical forcing.

Investigations of the sensitivity of the streamwise vortices in the natural jet to the static flaps, acting as surface roughness elements, will also be made as well as extending our investigation to the jet far field.

4. CONCLUSIONS

The present study investigates the development of three-dimensional vortical structures in order to shed some light on the mechanism behind an increased mixing in a controlled coaxial jet. Stereoscopic PIV applied in the cross-stream plane of the coaxial jet gives a unique possibility of exploring non-axisymmetric control modes and study the development and role of azimuthal instabilities and streamwise vortices in detail.

The results show that pairs of counter-rotating streamwise vortices are induced by amplification of secondary azimuthal instabilities in the inner and the outer shear layers.

The vortices are similar in both size and strength to the primary vortex rings, which emphasize their significance in the jet dynamics and their potential for mixing enhancement.

The presence of primary vortices, the appearance of streamwise vortices and the onset of mixing are strongly connected in both the natural coaxial jet and the axi-symmetrically controlled jet for a Strouhal number of unity.

The mean velocity profiles and the streamwise vortices develop faster when subjected to non-axisymmetric forcing modes, the least stable helical mode being superior in this sense, which suggests that the near-field mixing is even more enhanced.

However, for all the control modes, the helical mode develops further downstream and the differences in the mean velocity profiles become smaller.

Furthermore, the number of streamwise vortices increases in the downstream direction for all control modes and reaches a similar level roughly given by twice the azimuthal wavenumber.

In conclusion, the present results show that the number of streamwise vortices in the near field of a coaxial jet, and presumably also the mixing, can be flexibly controlled by applying different control modes, using individually-driven micro flap actuators.

ACKNOWLEDGEMENTS

JSPS and CREST are highly acknowledged for their financial support.

REFERENCES

1. C-. M. Ho and P. Huerre, Perturbed free shear layers, *Ann. Rev. Fluid Mech.,* vol. 16, pp. 205-234, 1984.
2. R.E. Breidenthal, Structure in turbulent mixing layers and wakes using a chemical reaction, *J. Fluid Mech.,* vol. 109, pp. 1-23, 1981.
3. S. E. Widnall, The instability of short waves on a vortex ring, *J. Fluid Mech.,* vol. 66, pp. 35-47, 1974.
4. R.T. Pierrehumbert and S.E Widnall, The two- and three-dimensional instabilities of a spatially periodic shear layer, *J. Fluid Mech.,* vol. 114, pp. 59-82, 19 82.
5. L.P. Bernal and A. Roshko, Streamwise vortex structure in plane mixing layers, *J. Fluid Mech.,* vol. 170, pp. 499-525, 1986.

6. J.C. Lasheras, J.S. Cho and T. Maxworthy, On the origin and evolution of streamwise vortical structures in a plane, free shear layer, *J. Fluid Mech.,* vol. 172, pp. 231-258, 1986.

7. J. E. Martin and E. Meiburg, Numerical investigation of three-dimensionally evolving jets subject to axisymmetric and azimuthal perturbations, *J. Fluid Mech.,* vol. 230, pp. 271-318, 1991.

8. J. E. Martin and E. Meiburg, Numerical investigation of three-dimensionally evolving jets under helical perturbations, *J. Fluid Mech.,* vol. 243, pp. 457-487, 1992.

9. D. Liepmann and M. Gharib, The role of streamwise vorticity in the near-field entrainment of round jets, *J. Fluid Mech.,* vol. 245, pp. 643-668, 1992.

10. W. J. A. Dahm, C. E. Frieler and G. Tryggvason, Vortex structure and dynamics in the near field of a coaxial jet, *J. Fluid Mech.,* vol. 241, pp. 371-402, 1992.

11. H. Rehab and E. Villermaux and E. J. Hopfinger, Flow regimes of large-velocity-ratio coaxial jets, *J. Fluid Mech.,* vol. 345, pp. 357-381, 1997.

12. E. Villermaux and H. Rehab, Mixing in coaxial jets, *J. Fluid Mech.,* vol. 425, pp. 161-185, 2000.

13. Y.-C. Chao and Y.-C. Jong and H.-W. Sheu, Helical mode exitation of lifted flames using piezoelectric actuators, *Exp. Fluids,* vol. 28, pp. 11-20, 2000.

14. C. B da Silva and G. Balarac and E. Me'tais, Transition in high velocity ratio coaxial jets analyzed form direct numerical simulation, *J. Turb.,* vol. 4, pp. 1-18, 2003.

15. N. Kurimoto, Y. Suzuki and N. Kasagi, Active control of coaxial jet mixing with arrayed micro actuators, *Transactions of the Japanese Society of Mechanical Engineers,* pp. 31-38, 2004.

16. J. Cohen and I. Wygnanski, The evolution of instabilities in the axisymmetric jet. Part 1. The linear growth of disturbances near the nozzle, *J. Fluid Mech.,* vol. 176, pp. 191-219, 1987.

17. M. Raffel and C. Willert and J. Kompenhans, *Particle Image Velocimetry A practical guide*, Springer-Verlag, 1998.

18. J. Westerweel, Fundamentals of digital particle image velocimetry, *Meas. Sci. Tech.,* vol. 8, pp. 1379-1392, 1997.

19. R. Keane and R. Adrian, Theory of cross-correlation in PIV, *Appl. Sci. Research,* vol. 49, pp. 191-215, 1992.

20. H. Suzuki, N. Kasagi and Y. Suzuki, Active control of an axisymmetric jet with distributed electromagnetic flap actuators, *Exp. Fluids,* vol. 36, pp. 498-509, 2004.